Structural and Nonstructural Viral Proteins Are Targets of T-Helper Immune Response against Human Respiratory Syncytial Virus*[S]

Elena Lorente‡, Alejandro Barriga‡, Eilon Barnea§, Carmen Mir‡, John A. Gebe¶, Arie Admon§, and Daniel López‡‖

Proper antiviral humoral and cellular immune responses require previous recognition of viral antigenic peptides that are bound to HLA class II molecules, which are exposed on the surface of antigen-presenting cells. The helper immune response is critical for the control and the clearance of human respiratory syncytial virus (HRSV) infection, a virus with severe health risk in infected pediatric, immunocompromised, and elderly populations. In this study, using a mass spectrometry analysis of complex HLA class II-bound peptide pools that were isolated from large amounts of HRSV-infected cells, 19 naturally processed HLA-DR ligands, most of them included in a complex nested set of peptides, were identified. Both the immunoprevalence and the immunodominance of the HLA class II response to HRSV were focused on one nonstructural (NS1) and two structural (matrix and mainly fusion) proteins of the infective virus. These findings have clear implications for analysis of the helper immune response as well as for antiviral vaccine design. ***Molecular & Cellular Proteomics 15: 10.1074/mcp.M115.057356, 2141–2151, 2016.***

Newly synthesized HLA class II molecules from antigen-presenting cells associate with the class II invariant chain (Ii). These complexes are eventually transported to specialized endosomal compartments where the Ii is progressively proteolyzed until only a fragment known as the class-II-associated invariant chain peptide (CLIP)[1] remains bound in the HLA class II peptide-binding groove to prevent it from binding to cellular peptides or pathogen peptides from the endogenous pathways. Interaction of HLA class II/CLIP complexes with the accessory molecule HLA-DM induces conformational changes in HLA class II molecules. Additionally, the release of CLIP results in peptide-receptive HLA class II molecules. This compartment fuses with a late endosome that contains exogenous proteins and/or viral particles that were previously endocytosed. Thus, the binding of antigen-processed peptides of different lengths, but with specific major anchor residues that can be deeply accommodated into specific pockets of the antigen recognition site of the HLA class II molecule, produces the stabilization of the nascent HLA class II/peptide complexes and allows for their subsequent transport to the cell membrane where they are exposed for T cell recognition (1).

Human respiratory syncytial virus (HRSV) (2), which is included in the *Paramyxoviridae* family of the Mononegavirales order, presents a single-stranded, negative-sense RNA genome that codes for 11 proteins. This enveloped pneumovirus causes repeat infections throughout life, and although in healthy adults mild infections are generally reported, the health risk in infected pediatric, immunocompromised, and elderly populations is much more serious. HRSV is the main cause of hospitalization for bronchiolitis and pneumonia in infants and young children, with infection rates approaching 70% in the first year of life (3). Worldwide, at least 3.4 million hospital admissions each year are associated with severe HRSV disease, and the global mortality rate was estimated at more than a quarter of a million deaths in 2010, mainly in developing countries (4).

The immune mechanisms involved in HRSV disease and protection are not completely understood; however, it is known that infection induces mucosal and systemic humoral and cellular responses. Studies evaluating $CD4^+$ and $CD8^+$ T-lymphocyte subsets individually or together showed that both effector MHC class I- and helper MHC class II-restricted cellular responses are particularly important in clearing infections (5). Previously, some HRSV epitopes that are restricted by different HLA class II molecules were identified using T cells from seropositive individuals (6–9). However, these experiments were performed with overlapping synthetic pep-

From the ‡Centro Nacional de Microbiología, Instituto de Salud Carlos III, 28220 Majadahonda (Madrid), Spain, §Department of Biology, Technion-Israel Institute of Technology, 32000 Haifa, Israel, ¶Benaroya Research Institute, Seattle, WA 98101, USA

Received December 7, 2015, and in revised form, April 13, 2016
Published, MCP Papers in Press, April 18, 2016, DOI 10.1074/mcp.M115.057356

Author contributions: D.L. designed research; E.L., A.B., E.B., C.M., and A.A. performed the research; J.A.G. contributed new reagents or analytic tools; E.L., A.B., and D.L. analyzed data; and D.L. wrote the paper.

[1] The abbreviations used are: CLIP, class II-associated invariant chain peptide; HRSV, human respiratory syncytial virus; HLA, human leukocyte antigen; HPLC, high performance liquid chromatography; IFN-γ, interferon-gamma; IL-4, interleukin 4; MHC, major histocompatibility complex; MS, mass spectrometry.

tides against only the F protein (6, 7) or a short fragment of 21 residues from the G protein (8). In contrast, only one published study attempted to elucidate the possible array of HRSV ligands that are restricted by HLA class II molecules in two different patients (9). These $CD4^+$ T cells, which were restricted by two HLA-DP alleles, were specific for two peptides from the matrix and attachment G proteins, respectively (9).

We are interested in the identification of viral ligands that are presented by several frequent HLA-DR class II molecules in HRSV-infected cells to analyze how the immune system selects natural HLA class II ligands and epitopes. The immunoproteomics analysis of HLA-DR ligands that were isolated from large amounts of healthy or HRSV-infected cells without any methodological bias (*e.g.* selection of an individual protein, use of HLA consensus scoring algorithms, etc.) demonstrated the existence of a diverse new naturally processed nested set of HLA-DR ligands from three different structural and nonstructural HRSV proteins in infected cells, as well as peptides that were recognized by specific T cells in an HLA-DR transgenic mouse model. This analysis defines both the nature and hierarchy of the T cell class-II-specific response against HRSV.

EXPERIMENTAL PROCEDURES

Mice—HLA-DRB1*0404 (10) transgenic mice were bred in our animal facilities in strict accordance with the recommendations of the *Guide for the Care and Use of Laboratory Animals* of the Spanish Comisión Nacional de Bioseguridad of the Ministerio de Medio Ambiente y Medio Rural y Marino (accreditation number 28079–34A). The protocol was approved by the Committee on Animal Experiment Ethics of the Institute of Health Carlos III (Permit Number: PI-283). All of the procedures were performed under isoflurane anesthesia, and all efforts were made to minimize suffering.

Synthetic Peptides—Peptides were purchased from Peptide 2.0 (Chantilly, VA). The correct molecular mass and composition of the peptides at > 90% purity was established by quadrupole ion trap microHPLC.

Preparation of cysteinylated peptides was achieved by peptide incubation (90 min at 37 °C) with a solution of aqueous ammonium hydroxide containing cysteine (0.29 mM). The reaction was terminated by acidifying the solution with glacial acetic acid. Oxidation was performed by incubation of the synthetic peptides with H_2O_2 (20 mM) for 90 min at 37 °C.

HRSV Infection of the Human JY Epstein–Barr-Transformed Cell Line—JY cells (HLA-DRB1*0404, –DRB4*0101, –DRB1*1301, and –DRB3*0101 or -DRB3*0201) were incubated with the HRSV Long strain and assayed at different time points for the presence of HRSV antigens using flow cytometry, as previously described, with either Epstein–Barr-transformed human B-cell lines (11) or other cell lines (12), to obtain a persistently infected JY-cell line that synthesized HRSV viral proteins and secreted infectious virus several months after infection (13).

HLA-Bound Peptide Isolation—HLA-bound peptides were isolated from 4×10^{10} healthy or HRSV-infected JY cells. The cells were lysed in 1% CHAPS (Sigma), 20 mM Tris/HCl buffer, and 150 mM NaCl, pH 7.5, in the presence of a protease inhibitor mixture. The HLA-DR/peptide complexes were isolated via affinity chromatography from the soluble cell extract fraction with the L243 (HB55) mAb, which is specific for a monomorphic pan-HLA-DR class II determinant (14). The HLA-bound peptides were eluted at 4 °C with 0.1% aqueous trifluoroacetic acid (TFA), separated from the large subunits, and concentrated with a Centricon 3 column (Amicon, Beverly, MA), exactly as previously described (13).

Electrospray-Ion Trap Mass Spectrometry Analysis—Peptide mixtures recovered after the ultrafiltration step were concentrated using Micro-Tip reversed-phase columns (C_{18}, 200 μl, Harvard Apparatus, Holliston, MA) (13). Each C_{18} tip was equilibrated with 80% acetonitrile in 0.1% TFA, washed with 0.1% TFA, and then loaded with the peptide mixture. The tip was then washed with an additional volume of 0.1% TFA, and the peptides were eluted with 80% acetonitrile in 0.1% TFA. The peptide samples were then concentrated to ~20 μl using vacuum centrifugation (13, 15).

The HLA class II peptides recovered from immunoprecipitated HLA-DR-specific mAb, were analyzed by μLC-MS/MS using an Orbitrap XL mass spectrometer (Thermo Scientific, San Jose, CA) that was fitted with a capillary HPLC (Eksigent, Dublin, CA) (13, 15). The peptides were resolved on homemade Reprosil C18-Aqua capillary columns (75 micron inner diameter) (16) with a 7–40% acetonitrile gradient for 2 h in the presence of 0.1% formic acid. The seven most intense masses that exhibited single-, double-, triple-, and quadruple-charge states were selected for fragmentation by CID from each full mass spectrum.

Database Searches—Raw mass spectrometry data were processed using Sequest 3.31 (Thermo-Fisher) (17) was used for peak-list generation from the μLC-MS/MS data. The peaks were identified using the Proteome Discoverer 1.0 SP1 (Thermo-Fisher) and Bioworks Browser 3.3.1 SP1 (Thermo-Fisher) software programs (17) using the human and virus parts of the NCBI database (Jan 2014), which included 776,554 proteins. The search was not limited by enzymatic specificity; the peptide mass tolerance was set to 0.005 Da, and the fragment ion tolerance was set to 0.5 Da (12, 13, 18). This search was not limited by any methodological bias (*e.g.* individual protein selection or HLA consensus scoring algorithm use). The identified peptides were selected if the following criteria were met: Sequest Xcorr >1.5 for singly, >2.5 for doubly, >3.2 for triply, and >4.3 for quadruply charged peptides, as well as a mass accuracy of 0.005 Da (12, 13, 18). The following variable modifications was also analyzed: cysteinilation (C), oxidation (M, P, H, F, Y, and W), methylation (C, and N terminus), and phosphorylation (Y, S, and T). When the MS/MS spectra fit more than one peptide, only the highest scoring peptide was selected. No viral peptides were found in a search of a reversed database. The purpose of the filtering criteria was to identify candidate HRSV peptide from the MS/MS scans for further manual inspection to determine whether the MS/MS fragment ion fingerprints matched the identified peptide sequences. Additionally, the corresponding synthetic peptide was made, and its MS/MS spectrum was used to confirm the assigned sequence. In addition, the false discovery rate was estimated by searching against the database with the reversed sequences. The maximum false discovery rate was set to 1%. The mass spectrometry data have been deposited to the MassIVE repository (https://massive.ucsd.edu) with the data set identifiers MSV000079650 and MSV000079647 for healthy and HRSV-infected cells, respectively.

In Silico Binding Prediction of HLA-DR Ligands—The predicted binding of each peptide to HLA-DR molecules was calculated using the artificial neural-network-based alignment method NetMHCIIpan (version 3.0) (19) (available in http://www.cbs.dtu.dk/services/NetMHCIIpan/) and the MHC-II binding prediction from IEDB (available in http://tools.iedb.org/mhcii/) (20). Strong and weak theoretical affinity of ligands to HLA-DR corresponding to $IC_{50} < 50$ nM and $50 \text{ nM} < IC_{50} < 500$ nM for NetMHCIIpan and < 1 and between 1 and 5 percentile ranks for IEDB were considered, respectively.

IL-4- and IFN-γ-Secreting Cell Detection by ELISPOT—ELISPOT assays to detect antigen-specific T cell activation were performed as

previously described (13). Briefly, either purified anti-mouse IL-4 (clone 11B11, Biolegend, San Diego, CA) or rat anti-mouse IFN-γ antibodies (clone R4–6A2, BD Pharmingen, San Diego, CA) were coated on 96-well MultiScreen HTS HA plates (Millipore, Billerica, MA). The plates were incubated overnight at room temperature and were blocked with medium that was supplemented with 10% fetal bovine serum for 2 h at 37 °C. Duplicate cultures of erythrocyte-depleted spleen cells were prepared from HLA-DR class II-transgenic mice at 7 days (acute response) post i.n. infection with 1×10^6 Long strain HRSV PFUs at different dilutions with 10^{-5} M peptide. The plates were incubated overnight at 37 °C in a 5% CO_2 atmosphere and were then washed with PBS-T (PBS 0.05% Tween-20). The plate wells were incubated for 2 h at room temperature with either biotinylated anti-mouse IL-4 (clone BVD6–24G2, Biolegend, San Diego, CA) or biotinylated anti-mouse IFN-γ mAbs (clone XMG1.2, BD Pharmingen, San Diego, CA), washed with PBS-T, and incubated for 1 h at room temperature with alkaline-phosphatase-conjugated streptavidin (Sigma, St. Louis, MO). The plates were additionally washed before adding the BCIP/NBT liquid substrate (Sigma, St. Louis, MO). To quantify the IL-4 or IFN-γ responses, wells were photographed using a Leica EZ4 HD stereo microscope and LAS EZ software (Leica Microsystems, Germany) and the spots were counted.

Experimental Design and Statistical Rationale—Previous analysis has shown that 4×10^{10} HRSV-infected human cells are sufficient to identity the HLA-bound viral peptide pool (13). Similar amounts of healthy human cells were used as negative control to discriminate viral and cellular peptides (included in proteome databases as well as unknown) and exclude erroneous assignments of viral peptides. Additionally, the corresponding synthetic viral sequence was made and its MS/MS spectrum was used to confirm the assigned sequence. Also, the false discovery rate was estimated by searching against the database with the reversed both viral and human sequences. To analyze the statistical significance of the assays, chi-square and unpaired Student's *t*-tests were used. p values < 0.05 were considered to be statistically significant.

RESULTS

The HLA-DR Peptidome from Healthy and Human HRSV-Infected Cells—The HLA-DR-bound peptide pool was isolated from large numbers of either healthy or HRSV-infected human cells. These peptide mixtures were subsequently separated by reversed-phase capillary HPLC and analyzed using mass spectrometry. MS analysis over a human proteome database resolved 728 fragmentation spectra as peptidic sequences of 201 human cellular proteins bound to HLA-DR molecules (Supplemental Table 1). As usual in HLA class II antigen processing, different nested sets of peptides with the same core and various N- and C-terminally extended residues were found (Supplemental Table 1). About half of them (354 peptides, the 49%) were identified from both healthy and human HRSV-infected cells. In contrast, the 35% and 16% of host-encoded peptides were detected only in healthy or human HRSV-infected cells extracts, respectively.

The peptide size of HLA-DR ligands followed a normal distribution (Fig. 1*A*), with an average length of 15 residues (8–33), within the standard HLA class II size range. No length differences were found between healthy and human HRSV-infected samples. Fig. 1*B* shows the predicted organelle location of these 201 proteins based on the Gene Ontology database (http://www.geneontology.org). Extracellular (18%), membrane (22%), and vesicles (20%) were the more relevant compartments. Other organelles associated with the endocytic pathway as Golgi and endoplasmic reticulum were the source of 7 and 6% of parental proteins, respectively. In total, proteins located in these five compartments of the endolyso-

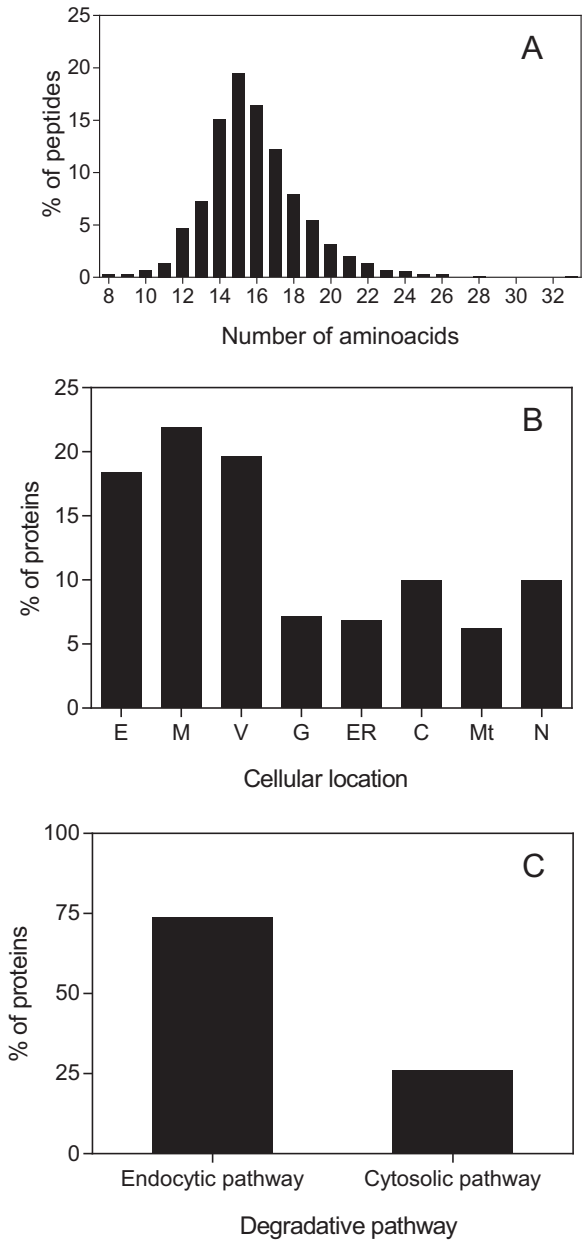

FIG. 1. **Size and intracellular distribution of HLA-DR cellular peptidome.** (*A*) Peptide size distribution of self-derived ligands. (*B*) Cellular location of the HLA-DR-associated peptide parental proteins; extracellular (E), membrane (Mb), vesicles: endosome/lysosome (V), Golgi (G), endoplasmic reticulum (ER), cytosol (C), mitochondria (Mt) or nuclear (N). (*C*) Percentage of HLA-DR ligands for each of the putative degradative pathways of the parental protein. Endocytic pathway includes E, Mb, V, G, and ER. The cytosolic pathway includes C, Mt, and N.

TABLE I
Summary of the HRSV ligands that were detected by MS/MS analysis in the HRSV persistently infected cells

Experimental mass[a]	ΔMass[b]	m/z	Sequence[c]	Protein	Position
1,508.88	0.002	3+	TDKLIHLTNALAKA	Nonstructural protein 1	31–44
1,721.03	0.002	3+	TDKLIHLTNALAKAVI	Nonstructural protein 1	31–46
1,858.09	0.002	3+	TDKLIHLTNALAKAVIH	Nonstructural protein 1	31–47
2,021.15	0.003	3+	YTDKLIHLTNALAKAVIH	Nonstructural protein 1	30–47
2,021.15	0.003	4+	YTDKLIHLTNALAKAVIH	Nonstructural protein 1	30–47
1,367.83	0.003	2+	ILVKQISTPKGPS	Matrix	57–69
1,580.94	0.002	3+	VNILVKQISTPKGPS	Matrix	55–69
1,580.94	0.001	2+	VNILVKQISTPKGPS	Matrix	55–69
1,694.02	0.002	2+	VNILVKQISTPKGPSL	Matrix	55–70
1,850.12	0.003	3+	VNILVKQISTPKGPSLR	Matrix	55–71
1,289.62	0.003	2+	LM*QSTPAANNRA	Fusion protein	96–107
1,701.86	0.001	2+	ELQLLM*QSTPAANNR	Fusion protein	92–106
1,772.89	0.003	2+	ELQLLM*QSTPAANNRA	Fusion protein	92–107
1,873.94	0.002	2+	TELQLLM*QSTPAANNRA	Fusion protein	91–107
1,159.67	0.002	1+	KAVVSLSNGVSV	Fusion protein	176–187
1,588.89	0.000	2+	TNKAVVSLSNGVSVLT	Fusion protein	174–189
1,675.92	–0.003	2+	TNKAVVSLSNGVSVLTS	Fusion protein	174–190
2,459.41	0.003	3+	STNKAVVSLSNGVSVLTSKVLDLK	Fusion protein	173–196
2,074.11	–0.002	3+	IDKQLLPIVNKQSC*RIS	Fusion protein	199–215
2,207.05	0.002	3+	TDVSSSVITSLGAIVSC*YGKT	Fusion protein	400–420
1,706.76	–0.004	2+	NRGIIKTFSNGC*DY	Fusion protein	428–441

[a] The monoisotopic ion mass in amu.
[b] The difference between nominal and experimentally detected monoisotopic ions in amu.
[c] Asterisks indicate oxidation of Met or cysteinylation of Cys.

somal pathway were predominant (74%, Fig. 1*C*). Proteins from cytosol (10%), mitochondria (6%), or nucleus (10%), corresponding to cytosolic pathway, were also detected (Figs. 1*B* and 1*C*). Newly, no significant differences were found between proteins identified from healthy and human HRSV-infected samples.

Physiological Processing Generated Multiple Different Viral HLA-DR Ligands in Human HRSV-Infected Cells—Using bioinformatics tools, different fragmentation spectra presented in the HRSV-infected HLA-bound peptide pool but absent from the control uninfected pool (data not shown) were resolved with high confidence parameters as HRSV protein peptides (Table I). Additionally, a human proteome database search failed to identify any of these spectra as human protein fragments, suggesting the viral origin of these peptides.

As cellular peptides, different nested sets of viral ligands with the same core and various N- and C-terminally extended residues were found. The first ion peak, with an *m/z* of 503.96, was assigned to the viral 14-mer sequence TDKLIHLTNALAKA, which spans residues 31–44 of the HRSV NS1 protein (Table I and Supplemental Fig. 1*A*). Four additional ion peaks with *m/z* of 574.68, 620.37, 506.29, and 674.72 were assigned to different viral amino acid sequences of the same HRSV NS1 protein that included the 31–44 minimal core with different C- (TDKLIHLTNALAKA**VI**, and TDKLIHLTNALAKA**VIH**) and N-terminally (**Y**TDKLIHLTNALAKA**VIH**) extended residues (Table I and Supplemental Figs. 1*B*-1*E*). Virtually all fragments with a relative abundance that was higher than 10% of the maximum signal of the five MS/MS spectra were assigned as daughter ions of the respective putative peptidic sequences (Supplemental Figs. 1*A*-1*E*). These theoretical assignments were confirmed by MS/MS spectrum identification of the corresponding synthetic peptide (Supplemental Figs. 1*A*-1*E*). It is remarkable that the 9-mer KLIHLTNAL peptide, which spans residues 33–41 of NS1 protein, was previously identified as the HLA-A*02 class I ligand (13, 21), suggesting that this region of the NS1 protein could be highly accessible to antigen processing.

Similarly, a nested set of natural ligands from the matrix (M) protein was also identified in the HLA-DR-bound peptide pool (Table I). The ILVKQISTPKGPS viral sequence, which spans residues 57–69, was the minimal core detected sequence, and N- (**VN**ILVKQISTPKGPS) and C-terminally (**VN**ILVKQISTPKGPS**L** and **VN**ILVKQISTPKGPS**LR**) extended ligands were also identified and confirmed with the corresponding synthetic peptide with all natural peptides identified in this study (Table I and Supplemental Figs. 1*F*-1*J*).

Additionally, multiple individual and nested sets of ligands from the fusion (F) protein were generated by antigen processing in the HRSV-infected cells. The first nested set included four natural ligands of different lengths that included the 91–107 region of the F protein (Table I). All of them were detected with an oxidation in their Met (Table I and Supplemental Figs. 1*K*-1*N*) because this residue easily oxidized in the peptide isolation and mass spectrometry analysis conditions (22). The second nested set comprised the 176–187 segment from the F protein as the minimal core and three different N- and C-terminally extended ligands (Table I and

Supplemental Figs. 1*O*-1*R*). Moreover, a ligand derived of 199–215 residues from this viral protein of the same F protein was also identified in the HLA-DR-bound peptide pool (Table I and Supplemental Fig. 1*S*). The Cys 212 of the F protein, which is present in this natural ligand, was detected because of the modification by cysteinylation, as a spontaneous non-enzymatic reaction where a Cys forms a disulfide bond to a free Cys molecule that (as the oxidation of Met) could be frequently incorporated *in vivo* and *in vitro* in the process of peptide isolation, as previously described (23). Finally, two other individual natural ligands spanning residues 400–420 and 428–441 from the F protein were identified and confirmed as the other viral sequences (Table I) that were also detected with Cys modification by cysteinylation (Supplemental Figs. 1*T* and 1*U*). Therefore, these results indicate that a total of 19 HLA-DR ligands, 16 of which were included in four different nested sets of peptides from the NS1, M, and F proteins, were processed and presented in HRSV-infected cells.

Theoretical Binding Affinity of the Viral Peptides and Allele Assignment—The JY cell line expresses the HLA-DR B1*0404, B4*0101, B1*1301, and B3*0101 or B3*0201 chains. Thus, prediction of peptide binding to the viral ligands to each HLA-DR molecule was confirmed using two different computational approaches (Table II). The NetMHCIIpan neural-network-based alignment method suggests that most ligands ($NS1_{30-47}$, M_{55-71}, F_{91-107}, $F_{173-196}$, and $F_{199-215}$) could be bound with different affinities to all HLA-DR molecules that are expressed by the JY cell line, except HLA-DRB3*0101. Additionally, the $F_{400-420}$ ligand could also be presented by the B1*0404, B1*1301, and B3*0201 class II molecules. In contrast, the NetMHCIIpan did not predict binding of the $F_{428-441}$ peptide to different considered HLA-DR molecules.

The consensus approach from IEDB was more selective with the different antigen-presenting molecules, suggesting that all HLA-DR ligands identified could be presented with different affinities to the B1*0404 molecule. In contrast, B4*0101 and B1*1301 could only bind the M_{55-71}, F_{91-107}, and $F_{199-215}$ regions, and B3*0201 would be the most restrictive allele with only two possible ligands: $NS1_{30-47}$, and F_{91-107}. As in a previous algorithm, the IEDB bioinformatics tool failed to predict the binding of all ligands that were detected by mass spectrometry to HLA-DRB3*0101.

HLA class II binding prediction from these three viral proteins (NS1, M, and F) by NetMHCIIpan and IEDB computational tools indicates 5 and 10 strong binding peptides, respectively. Only a partial correlation between this theoretical analysis and experimental detection of HLA-DR ligands ($NS1_{30-47}$, and F_{91-107} for NetMHCIIpan and $NS1_{30-47}$, F_{91-107}, and $F_{199-215}$ for IEDB) was found.

Both bioinformatics tools predicted that most ligands that were identified by mass spectrometry in this study could bind up to four different HLA-DR molecules. This promiscuity in

TABLE II

Theoretical affinity to HLA-DR of the HRSV ligands that were detected by MS/MS analysis in the HRSV persistently infected cells

Peptide	Sequence	HLA-DR allele									
		B1*0404		B4*0101		B1*1301		B3*0101		B3*0201	
		NetMHCIIpan	IEDB	NetMHCIIpan	IEDB	NetMHCIIpan	IEDB	NetMHCIIpan	IEDB	NetMHCIIpan	IEDB
$NS1_{30-47}$	YTDKLIHLTNALAKAVIH	++[a]	++[b]	++	–	++	–	–	–	++	++
M_{55-71}	VNILVKQISTPKGPSLR	+	+	+	++	+	++	–	–	+	–
F_{91-107}	TELQLLMQSTPAANNRA	++	++	+	+	+	+	–	–	++	+
$F_{173-196}$	STNKAVVSLSNGVSVLTSKVLDLK	+	+	+	–	+	–	–	–	+	–
$F_{199-215}$	IDKQLLPIVNKQSCRIS	+	++	+	+	+	++	–	–	+	–
$F_{400-420}$	TDVSSSVITSLGAIVSCYGKT	+	+	–	–	+	–	–	–	+	–
$F_{428-441}$	NRGIIKTFSNGCDY	–	+	–	–	–	–	–	–	–	–

[a] As calculated in the NetMHCIIpan-3.0 server. The threshold for strong (++) and weak (+) binding peptides was 50 and 500 nM, respectively.

[b] As calculated in the Immuno Epitope Database server. The threshold for strong (++) and weak (+) binding peptides was 1 and 5 of the percentile rank, respectively.

FIG. 2. **Location of different HLA-DR ligands in the crystal structures of the HRSV fusion protein.** The HRSV fusion protein homotrimer crystal structure from the Protein Data Bank 4ZYP was determined (25). Green cartoons represent the protein backbone with the following color scheme for the HLA-DR ligands that were identified by mass spectrometry: F_{91-107} (cyan), $F_{173-196}$ (blue), $F_{199-215}$ (magenta), $F_{400-420}$ (red), and $F_{428-441}$ (yellow). The figure was prepared using the PyMOL program.

MHC class II binding, which is far from being an exception, could be relatively common (24).

A Significant Fraction of the Viral Proteome, Which Was Mainly Focused on the F Protein, Was Monitored in Association with the HLA-DR Class II Molecules—The Long strain HRSV proteome contains 4,402 residues. Thus, the seven long nested set ligands that were detected by mass spectrometry represent 3% of the viral proteome. Additionally, five of these ligands were derived from the F protein, and the 93 residues included in these ligands represent 16% of the F protein sequence. Thus, this high percentage of "immune coverage" suggests a high cellular immune pressure that was focused on the F protein.

Most of the HLA-DR Ligands from the F Protein Are Accessible to Direct Interaction with MHC Class II Molecules—Next, the accessibility of each different F protein HLA class II ligands that are identified by mass spectrometry from HRSV-infected cells was analyzed. As is typical for all Paramyxoviridae, the F protein assembles into a homotrimer, the crystal structure of which is available in the Protein Data Bank as 4ZYP (25). Thus, each identified ligand is shown three times in Fig. 2.

All HRSV F protein HLA class II ligands, except the $F_{400-420}$ peptide (depicted in red) that was covered by the $F_{428-441}$ ligand (yellow), were located in the exposed regions of the respective crystal structure, as shown in Fig. 2, and were thus accessible to direct interaction with HLA-DR molecules.

*The Recognition of HLA-DR Ligands by Specific T Cells in HRSV-Infected HLA-DRB1*0404 Transgenic Mice*—To study *in vivo* the physiological relevance of the identified HLA class II viral ligands, HLA-DRB1*0404 transgenic mice were infected with HRSV; other mice were not available. Later, a physiological measurement of the functional *ex vivo* activity of T cells against the different HLA class II viral ligands that were identified using mass spectrometry was carried out. Spleen cells specifically recognized cells pulsed with each one of the seven peptides corresponding to the longest ligand of each nested set of the identified viral ligands, and they were simultaneously recognized as part of the acute response to HRSV (Fig. 3).

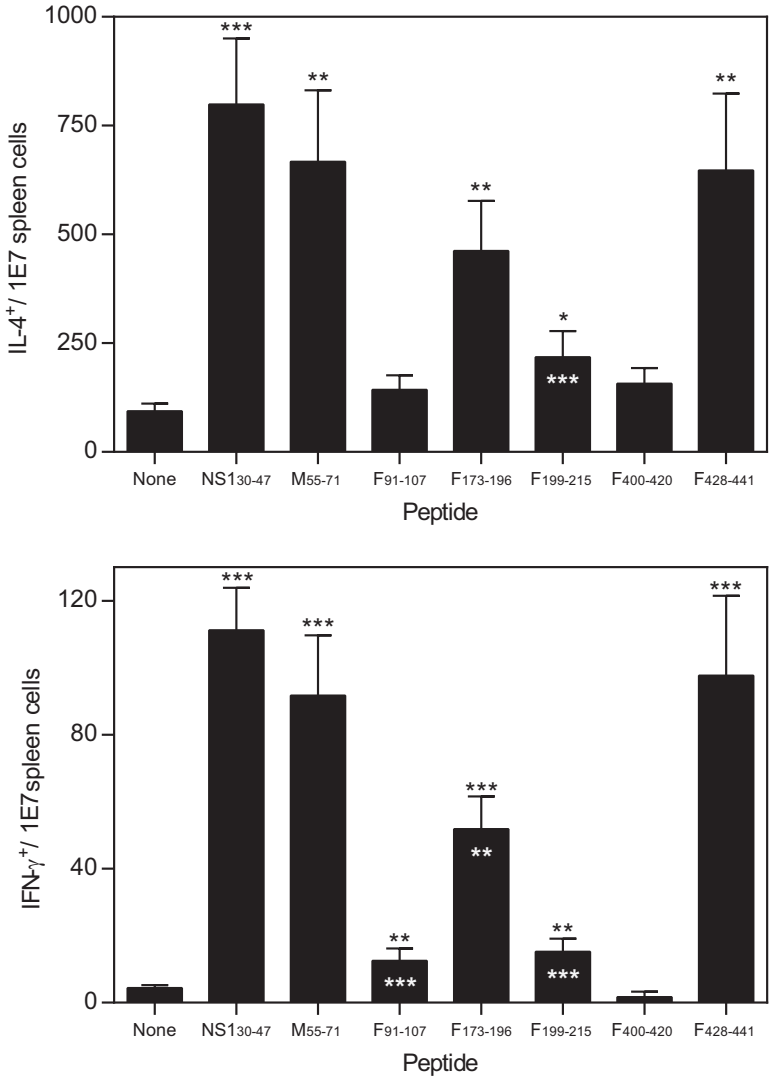

FIG. 3. **The immunogenicity of HRSV-derived HLA class II-restricted peptides in the HLA-DR transgenic mice.** HLA-DRB1*0404 spleen cells that were pulsed with the indicated HRSV-synthetic peptides were analyzed by ELISPOT for T cell activation and were measured as the number of IL-4- (*upper panel*) and IFN-γ-secreting cells (*bottom panel*). The HRSV-specific splenocytes were obtained from HLA-DRB1*0404 transgenic mice that were immunized for 7 days (acute response) post HRSV infection. The results were calculated as the mean of four to five (IL-4) and eight to ten (IFN-γ) independent experiments ± S.D. Significant *p* values: *, $p < 0.05$, **, $p < 0.01$, and ***, $p < 0.001$ *versus* a negative control (black asterisks) or *versus* the $NS1_{30-47}$ ligand (white asterisks) are indicated.

Four ligands ($NS1_{30-47}$, M_{55-71}, $F_{173-196}$, and $F_{428-441}$) that were detected displayed IL-4^+ responses of the same order, the $F_{199-215}$ natural peptide was weakly but significantly recognized, whereas the F_{91-107}, and $F_{400-420}$ peptides were negative (Fig. 3*A*). In contrast, the IFN-γ^+ responses in the HLA-DRB1*0404 transgenic mice were more diverse. The $NS1_{30-47}$, M_{55-71}, and $F_{428-441}$ epitopes were similarly recognized, the $F_{173-196}$ ligand showed an intermediate response, the F_{91-107}, and $F_{199-215}$ peptides were weakly but significantly recognized, and only the $F_{400-420}$ peptide was not recognized by specific T cells from these transgenic mice (Fig. 3*B*). Additionally, for each nested set of ligands, both the shortest and longest peptides were recognized equally by the HRSV-infected transgenic mouse T cells (data not shown). Therefore, five peptides induced Th1 and Th2 cytokine expression, but two more only induced Th2 cytokine expression in spleen cells from the HRSV-infected mice.

While IL-4 secretion is mediated by MHC class II molecules, IFN-γ^+ responses can result from either class I or II-specific recognition. Thus, the IFN-γ secretion was assayed in the presence of anti-HLA-DR mAb (Fig. 4). Specific recognition of target cells that were prepulsed with each one of these six long epitopes was totally inhibited by the specific anti-DR mAb (Fig. 4). In contrast, the activity of antiviral IFN-γ-secreting cells against two other HRSV epitopes that were previously identified as MHC class I restricted ($M_{188-195}$ (26) and $F_{250-258}$ (27)) was not altered in the same transgenic mice in the presence of this HLA class II mAb (Fig. 4). These results demonstrate that the six ligands were functional HLA-DRB1*0404-restricted epitopes.

The IEDB bioinformatics tool predicted that the seven ligands that were eluted from HRSV-infected cells could be bound to HLA-DRB1*0404 molecule (Table II), and all of them, except the $F_{400-420}$ peptide, were recognized in this transgenic mouse model. The absence of the $F_{400-420}$ peptide recognition did not formally exclude that this peptide could be an HLA-DRB1*0404 ligand because several factors (TCR repertoire or regulatory T cells, among others) can condition

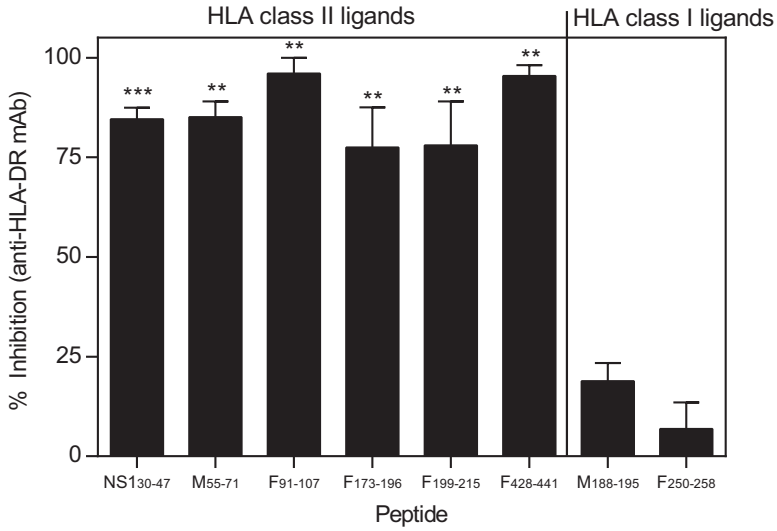

FIG. 4. **Inhibition of IFN-γ secretion of T cells by the anti-HLA-DR mAb, L243 (HB55), in the HLA class II transgenic mice.** HLA-DRB1*0404 spleen cells, which were pulsed with the indicated HLA class II or I-restricted HRSV-synthetic peptides, were incubated with the anti-HLA-DR mAb, L243 (HB55) and later analyzed for IFN-γ-secreting cell detection, as in Fig. 3. The results were calculated as the mean of three to five independent experiments $\pm$ S.D. Significant p values: **, $p < 0.01$, and ***, $p < 0.001$ *versus* the respective peptide without mAb are indicated.

the antigen presentation of peptides that are efficiently bound to MHC molecules. The prediction of the NetMHCIIpan method was slightly worse because the proficiently presented $F_{428-441}$ epitope was predicted as not an HLA-DRB1*0404 ligand (Table II). Thus, both bioinformatics tools were reasonably accurate in their predictions for this DRB1*0404 molecule, and thus, these data suggest that most of the seven ligands that were identified by mass spectrometry in this study could be presented by one or more of the three additional HLA-DR molecules that were expressed in the JY cell line (Table II), and they might be recognized by specific T cells.

DISCUSSION

Three major issues could be derived from the results reported here about the nature and hierarchy of the T cell class-II-specific response against HRSV.

First, although it is commonly assumed that the MHC class II ligands are generated in a first step by proteolytic activity of lysosomal proteases on the protein antigens and later the resulting peptides bind to MHC class II molecules, this "cut/trim first, bind later" model is inherently problematic because proteolytic fragments are rare and short lived in the terminal degradative lysosome environment. A second "bind first, cut/trim later" model, in opposition, proposes that MHC class II molecules scan the protein antigens to find the best-fitting epitopes and later lysosomal proteases acting on MHC class II-bound antigens trim the protruding ends that are unprotected by MHC class II molecules to release the protein antigen ligand. Both models, and the different studies supporting each one, are reviewed in (28). A recent study using a reductionist cell-free antigen processing system of *in vitro* interactions with MHC class II molecules, cathepsins, and protein antigens suggests that both hypotheses could not necessarily be mutually exclusive, and according to this reductive study, autoantigens follow the first model whereas pathogen-derived proteins could be processed according the bind first, cut/trim later model.

Therefore, the bind first, cut/trim later model implies that the ligands must be exposed to allow the direct interaction with MHC class II molecules. Our results indicate that five of six HLA class II ligands from HRSV F protein were located in the exposed regions of this viral protein and were thus accessible to solvent and direct interaction with HLA-DR molecules. These data would be compatible with the bind first, cut/trim later model for MHC class II pathogen-derived epitopes. On the other hand, the environment in the lysosomal compartment with it low pH could be sufficiently denaturative to allow unfolding of the protein and its binding to the HLA class II molecules of protected domains in the protein.

Second, unlike the class I immune response previously described (13), the immunoprevalence and immunodominance of the HLA class II responses were not limited by the HRSV viral transcription group. The HRSV genome contains 10 genes in the following order: 3′ NS1-NS2-N-P-M-SH-G-F-M2/M2–2-L (Fig. 5). These genes are transcribed sequentially as a mRNA synthesis gradient that is inversely proportional to the distance of the gene from the 3′ end of the genome, and thus the promoter-proximal genes are expressed more efficiently (29). As for the other viruses that belong to the Mononegavirales order, the HRSV genome has been divided into three different mRNA expression level groups (30): 3′ core protein genes; intermediate (IM) genes; and 5′ large polymerase gene, which involve 26% (NS1, NS2, N, P, and M proteins), 25% (SH, G, F, M2, and M2–2 proteins), and 49% (L protein) of the viral proteome, respectively (Fig. 5). In previous immunoproteomics studies (12, 13, 26), analyses of the HLA class I-restricted antiviral immune response against HRSV identified 16 natural viral ligands by mass spectrometry. This analysis showed that 12 of the HRSV ligands that were detected were included in proteins encoded by the 3′ group, whereas only three and one of them were integrated into proteins that were encoded by the intermediate and 5′ groups, respectively (Fig. 5). The quantification of the overall T

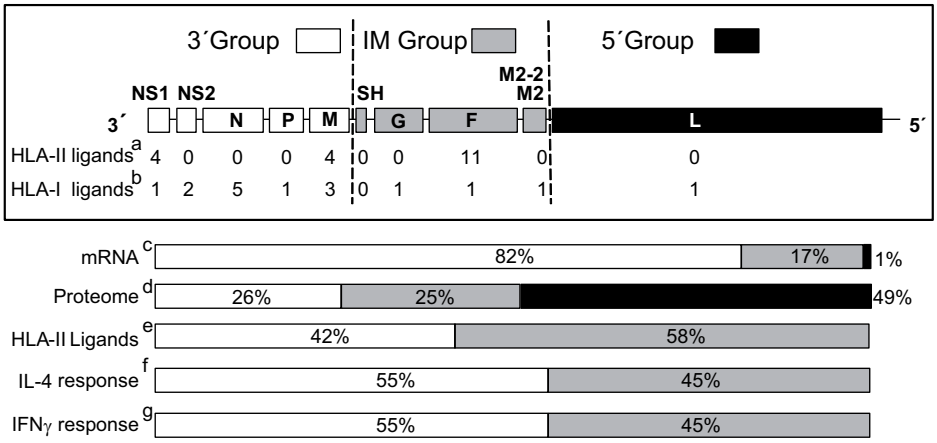

FIG. 5. **HLA class II ligands identified by mass spectrometry and their relation with the HRSV genome, mRNA, proteome, and T cell immune response.** Schematic representation of the HRSV genome indicating the three different transcription groups (3′, intermediate or IM, and 5′) encoding the viral proteome separated by dotted lines is shown. The abbreviations used for viral proteins are NS1 (nonstructural protein 1), NS2 (nonstructural protein 2), N (nucleoprotein), P (phosphoprotein), M (matrix protein), SH (small hydrophobic protein), G (glycoprotein), F (fusion protein), M2 (matrix protein 2), M2–2 (matrix protein 22k), and L (polymerase). For each transcription group, the number of HLA class II ligands that were identified by mass spectrometry in this report are shown in [a]. The HLA class I ligands that were identified by mass spectrometry in previous studies (12, 13, 26) are shown in [b]. The transcription gradient, which was measured as the mRNA molar ratio percentage (29, 34, 35) is shown in [c]. The proteome percentage is shown in [d]. The HLA class II ligand percentage from the total is shown in [e]. The total IL-4$^+$ or IFN-γ^+ immune response percentage that was detected in the HLA class II-transgenic mice is shown in [f] and [g], respectively.

cell responses that were specific for the epitopes presented by the different HLA class I molecules showed that most (91%) of the specific analyzed T cell responses were restricted by ligands from proteins that were encoded by the 3′ group (13). These results indicated that the proteins to which HLA class I antigen processing and presentation were addressed, that is, the immunoprevalence and immunodominance of the HLA class I response, were determined by the HRSV transcription groups.

In the current study, 19 natural HRSV ligands (four4 from NS1 protein, four other derived from matrix protein, and 11 encoded from F gene) were identified and associated with HLA-DR molecules. These HLA class II ligands found in the immunoproteomics analysis could be grouped in an 8:11:0 (3′:IM:5′) distribution that is significantly different to the 12:3:1 distribution of the HLA class I ligands that was described previously (p value = 0.04) as well as an expected random distribution (4:4:8) along the viral proteome (p value = 0.002). Therefore, in contrast to the HLA class I-restricted response, the immunoprevalence of the HLA-DR response was not limited by the HRSV transcription groups.

Additionally, quantification of the overall T cell responses that were specific for the six epitopes presented by the HLA-DRB1*0404 molecule showed that the specific analyzed IL-4$^+$ and IFN-γ^+ responses were restricted against ligands from the NS1 (30%) and M (25%) proteins, which are proteins that are encoded by the 3′ group, and from the F (45%) protein encoded by the intermediate group (Fig. 5). Thus, the F protein, which only corresponds with the 13% of viral proteome, was the main target of the HLA class II-restricted response; however, ligands from the NS1 and M proteins were also significantly presented and recognized. These differences between HLA class I and II immunoprevalence and immunodominance are associated with the different antigen processing pathways, whereas the HLA class I ligands are generated mainly by proteolytic processing of newly synthesized viral proteins in the cytosol; nevertheless, the peptides bound to the HLA class II molecules were mainly derived from proteins or viral particles that were endocytosed and later degraded in endosomes by acid-dependent proteases. However, NS1 is a nonstructural protein of HRSV that interacts with multiple intracellular proteins (31) and thus should not be presented via the classical HLA class II antigen presentation pathway. Additionally, an HRSV NS2 epitope that was restricted by the murine MHC class II molecule I-E^d was previously described (32). Altogether, these data indicate that alternative MHC class II antigen presentation pathways must be functional in HRSV-infected cells. In recent years, several examples of endogenous MHC class II presentation involving different mechanisms (*e.g.* macroautophagy and chaperone-mediated autophagy) have been described (summarized in (33)). Thus, some of these additional nonclassical MHC class II antigen-processing pathways must generate the four HLA-DR ligands derived from NS1 protein in HRSV-infected cells.

And lastly, the analysis of the immunoprevalence and immunodominance of the HLA class II response described in this report together with the HLA class I response from previous immunoproteomics studies (12, 13, 26) could have implications for vaccine development. The 3′ core and intermediate genes translate 52% of the HRSV proteome; however, they include 94% and 100% of natural HLA class I and II

ligands identified in the diverse immunoproteomics studies, respectively (Fig. 5). Additionally, the proteins encoded by these genes are responsible for 97% and 100% of cellular immune response against HRSV (Fig. 5). The HRSV Long strain proteome contains 4,402 residues; thus, these two transcription groups encoded for 2,237 residues, which would be a construct that is perhaps too large for their inclusion in a vaccine. Nevertheless, a therapeutic immunogen (*e.g.* DNA plasmid or recombinant vaccinia) expressing the four viral (NS1, N, M, and F) proteins against which these HLA immune responses are mainly targeted represents only 1,358 residues, namely 31% of viral proteome; however, almost all of the antiviral T cell responses that were mediated by several frequent HLA class I and II alleles were preserved (92% and 100%, respectively). Finally, this therapeutic design could be easily extrapolated for other Paramyxoviridae family members and perhaps also for the other Mononegavirales order viruses such as the Filovirus because they all share the same genomic structure, although future and extensive studies with individual viruses of this order are needed.

Acknowledgments—The excellent technical assistance of M. Jiménez, F. Lasala and the Centro Nacional de Microbiología animal facility is gratefully acknowledged.

* This work was supported by the Spanish Ministry of Economy grants BIO2011–25636 to D.L. and to A. A. from the ISF 916/05. The funding agencies had no role in the study design, data collection, analysis decision to publish, or preparation of the manuscript. We had no conflicting financial interests.

[S] This article contains supplemental material Supplemental Table 1 and Supplemental Fig. 1.

‖ To whom correspondence should be addressed: Unidad de Inmunología Viral, Centro Nacional de Microbiología, Instituto de Salud Carlos III, 28220 Majadahonda (Madrid), Spain, Tel.: +34 91 822 37 08, Fax: +34 91 509 79 19; E-mail: dlopez@isciii.es.

REFERENCES

1. Blum, J. S., Wearsch, P. A., and Cresswell, P. (2013) Pathways of antigen processing.*Annu. Rev. Immunol.* **31,** 443–473
2. Collins, P. L., Chanock, R. M., and Murphy, B. R. (2007) Respiratory syncytial virus. In Knipe, D. M., and Howley, P. M., eds. *Fields Virology*, Lippincott Williams & Wilkins, Philadelphia, PA.,
3. Glezen, P., and Denny, F. W. (1973) Epidemiology of acute lower respiratory disease in children. *N. Engl. J. Med.* **288,** 498–505
4. Lozano, R., Naghavi, M., Foreman, K., Lim, S., Shibuya, K., Aboyans, V., Abraham, J., Adair, T., Aggarwal, R., Ahn, S. Y., Alvarado, M., Anderson, H. R., Anderson, L. M., Andrews, K. G., Atkinson, C., Baddour, L. M., Barker-Collo, S., Bartels, D. H., Bell, M. L., Benjamin, E. J., Bennett, D., Bhalla, K., Bikbov, B., Bin Abdulhak, A., Birbeck, G., Blyth, F., Bolliger, I., Boufous, S., Bucello, C., Burch, M., Burney, P., Carapetis, J., Chen, H., Chou, D., Chugh, S. S., Coffeng, L. E., Colan, S. D., Colquhoun, S., Colson, K. E., Condon, J., Connor, M. D., Cooper, L. T., Corriere, M., Cortinovis, M., de Vaccaro, K. C., Couser, W., Cowie, B. C., Criqui, M. H., Cross, M., Dabhadkar, K. C., Dahodwala, N., De Leo, D., Degenhardt, L., Delossantos, A., Denenberg, J., Des Jarlais, D. C., Dharmaratne, S. D., Dorsey, E. R., Driscoll, T., Duber, H., Ebel, B., Erwin, P. J., Espindola, P., Ezzati, M., Feigin, V., Flaxman, A. D., Forouzanfar, M. H., Fowkes, F. G., Franklin, R., Fransen, M., Freeman, M. K., Gabriel, S. E., Gakidou, E., Gaspari, F., Gillum, R. F., Gonzalez-Medina, D., Halasa, Y. A., Haring, D., Harrison, J. E., Havmoeller, R., Hay, R. J., Hoen, B., Hotez, P. J., Hoy, D., Jacobsen, K. H., James, S. L., Jasrasaria, R., Jayaraman, S., Johns, N., Karthikeyan, G., Kassebaum, N., Keren, A., Khoo, J. P., Knowlton, L. M., Kobusingye, O., Koranteng, A., Krishnamurthi, R., Lipnick, M., Lipshultz, S. E., Ohno, S. L., Mabweijano, J., MacIntyre, M. F., Mallinger, L., March, L., Marks, G. B., Marks, R., Matsumori, A., Matzopoulos, R., Mayosi, B. M., McAnulty, J. H., McDermott, M. M., McGrath, J., Mensah, G. A., Merriman, T. R., Michaud, C., Miller, M., Miller, T. R., Mock, C., Mocumbi, A. O., Mokdad, A. A., Moran, A., Mulholland, K., Nair, M. N., Naldi, L., Narayan, K. M., Nasseri, K., Norman, P., O'Donnell, M., Omer, S. B., Ortblad, K., Osborne, R., Ozgediz, D., Pahari, B., Pandian, J. D., Rivero, A. P., Padilla, R. P., Perez-Ruiz, F., Perico, N., Phillips, D., Pierce, K., Pope, C. A., 3rd, Porrini, E., Pourmalek, F., Raju, M., Ranganathan, D., Rehm, J. T., Rein, D. B., Remuzzi, G., Rivara, F. P., Roberts, T., De León, F. R., Rosenfeld, L. C., Rushton, L., Sacco, R. L., Salomon, J. A., Sampson, U., Sanman, E., Schwebel, D. C., Segui-Gomez, M., Shepard, D. S., Singh, D., Singleton, J., Sliwa, K., Smith, E., Steer, A., Taylor, J. A., Thomas, B., Tleyjeh, I. M., Towbin, J. A., Truelsen, T., Undurraga, E. A., Venketasubramanian, N., Vijayakumar, L., Vos, T., Wagner, G. R., Wang, M., Wang, W., Watt, K., Weinstock, M. A., Weintraub, R., Wilkinson, J. D., Woolf, A. D., Wulf, S., Yeh, P. H., Yip, P., Zabetian, A., Zheng, Z. J., Lopez, A. D., Murray, C. J., Al Mazroa, M. A., Memish, Z. A. (2012) Global and regional mortality from 235 causes of death for 20 age groups in 1990 and 2010: A systematic analysis for the Global Burden of Disease Study 2010. *Lancet* **380,** 2095–2128
5. Graham, B. S., Bunton, L. A., Wright, P. F., and Karzon, D. T. (1991) Role of T lymphocyte subsets in the pathogenesis of primary infection and rechallenge with respiratory syncytial virus in mice. *J. Clin. Invest.* **88,** 1026–1033
6. Levely, M. E., Bannow, C. A., Smith, C. W., and Nicholas, J. A. (1991) Immunodominant T-cell epitope on the F protein of respiratory syncytial virus recognized by human lymphocytes. *J. Virol.* **65,** 3789–3796
7. van Bleek, G. M., Poelen, M. C., van der Most, R., Brugghe, H. F., Timmermans, H. A., Boog, C. J., Hoogerhout, P., Otten, H. G., and van Els, C. A. (2003) Identification of immunodominant epitopes derived from the respiratory syncytial virus fusion protein that are recognized by human CD4 T cells. *J. Virol.* **77,** 980–988
8. Yusibov, V., Mett, V., Mett, V., Davidson, C., Musiychuk, K., Gilliam, S., Farese, A., Macvittie, T., and Mann, D. (2005) Peptide-based candidate vaccine against respiratory syncytial virus. *Vaccine* **23,** 2261–2265
9. de Waal L., Yüksel, S., Brandenburg, A. H., Langedijk, J. P., Sintnicolaas, K., Verjans, G. M., Osterhaus, A. D., and de Swart, R. L. (2004) Identification of a common HLA-DP4-restricted T-cell epitope in the conserved region of the respiratory syncytial virus G protein. *J. Virol.* **78,** 1775–1781
10. Gebe, J. A., Unrath, K. A., Falk, B. A., Ito, K., Wen, L., Daniels, T. L., Lernmark, A., and Nepom, G. T. (2006) Age-dependent loss of tolerance to an immunodominant epitope of glutamic acid decarboxylase in diabetic-prone RIP-B7/DR4 mice. *Clin. Immunol.* **121,** 294–304
11. Bangham, C. R., and McMichael, A. J. (1986) Specific human cytotoxic T cells recognize B-cell lines persistently infected with respiratory syncytial virus. *Proc. Natl. Acad. Sci. U.S.A.* **83,** 9183–9187
12. Infantes, S., Lorente, E., Barnea, E., Beer, I., Cragnolini, J. J., García, R., Lasala, F., Jiménez, M., Admon, A., and López, D. (2010) Multiple, non-conserved, internal viral ligands naturally presented by HLA-B27 in human respiratory syncytial virus-infected cells. *Mol. Cell Proteomics* **9,** 1533–1539
13. Johnstone, C., Lorente, E., Barriga, A., Barnea, E., Infantes, S., Lemonnier, F. A., David, C. S., Admon, A., and López, D. (2015) The Viral Transcription Group determines the HLA class I cellular immune response against human respiratory syncytial virus. *Mol. Cell Proteomics* **14,** 893–904
14. Lampson, L. A., and Levy, R. (1980) Two populations of Ia-like molecules on a human B cell line. *J. Immunol.* **125,** 293–299
15. Lorente, E., Infantes, S., Barnea, E., Beer, I., García, R., Lasala, F., Jimenez, M., Vilches, C., Lemonnier, F. A., Admon, A., and López, D. (2012) Multiple viral ligands naturally presented by different class I molecules in transporter antigen processing-deficient vaccinia virus-infected cells. *J. Virol.* **86,** 527–541
16. Ishihama, Y., Rappsilber, J., Andersen, J. S., and Mann, M. (2002) Microcolumns with self-assembled particle frits for proteomics. *J. Chromatogr. A* **979,** 233–239
17. Eng, J., McCormack, A., and Yates, J. (2009) An approach to correlate tandem mass spectral data of peptides with amino acid sequences in a protein database. *J. Amer. Soc. Mass. Spectr.* **5,** 976–989
18. Lorente, E., Infantes, S., Barnea, E., Beer, I., García, R., Lasala, F., Jimenez,

M., Admon, A., and López, D. (2011) TAP-independent human histocompatibility complex-Cw1 antigen processing of an HIV envelope protein conserved peptide. *AIDS* **25,** 265–269
19. Karosiene, E., Rasmussen, M., Blicher, T., Lund, O., Buus, S., and Nielsen, M. (2013) NetMHCIIpan-3.0, a common pan-specific MHC class II prediction method including all three human MHC class II isotypes, HLA-DR, HLA-DP and HLA-DQ. *Immunogenetics* **65,** 711–724
20. Wang, P., Sidney, J., Dow, C., Mothé, B., Sette, A., and Peters, B. (2008) A systematic assessment of MHC class II peptide binding predictions and evaluation of a consensus approach. *PLoS Comput. Biol.* **4,** e1000048
21. Meiring, H. D., Soethout, E. C., Poelen, M. C., Mooibroek, D., Hoogerbrugge, R., Timmermans, H., Boog, C. J., Heck, A. J., de Jong, A. P., and van Els, C. A. (2006) Stable isotope tagging of epitopes: A highly selective strategy for the identification of major histocompatibility complex class I-associated peptides induced upon viral infection. *Mol. Cell Proteomics.* **5,** 902–913
22. López, D., Calero, O., Jiménez, M., García-Calvo, M., and Del Val, M. (2006) Antigen processing of a short viral antigen by proteasomes. *J. Biol. Chem.* **281,** 30315–30318
23. Mommen, G. P., Frese, C. K., Meiring, H. D., van Gaans-Van den Brink, de Jong, A. P., van Els, C. A., and Heck, A. J. (2014) Expanding the detectable HLA peptide repertoire using electron-transfer/higher-energy collision dissociation (EThcD). *Proc. Natl. Acad. Sci. U.S.A.* **111,** 4507–4512
24. Consogno, G., Manici, S., Facchinetti, V., Bachi, A., Hammer, J., Conti-Fine, B. M., Rugarli, C., Traversari, C., and Protti, M. P. (2003) Identification of immunodominant regions among promiscuous HLA-DR-restricted CD4+ T-cell epitopes on the tumor antigen MAGE-3. *Blood* **101,** 1038–1044
25. Gilman, M. S., Moin, S. M., Mas, V., Chen, M., Patel, N. K., Kramer, K., Zhu, Q., Kabeche, S. C., Kumar, A., Palomo, C., Beaumont, T., Baxa, U., Ulbrandt, N. D., Melero, J. A., Graham, B. S., and McLellan, J. S. (2015) Characterization of a prefusion-specific antibody that recognizes a quaternary, cleavage-dependent epitope on the RSV fusion glycoprotein. *PLoS Pathol.* **11,** e1005035
26. Infantes, S., Lorente, E., Cragnolini, J. J., Ramos, M., García, R., Jiménez, M., Iborra, S., Del Val, M., and López, D. (2011) Unusual viral ligand with alternative interactions is presented by HLA-Cw4 in human respiratory syncytial virus-infected cells. *Immunol. Cell Biol.* **89,** 558–565
27. Johnstone, C., Ramos, M., Garcia-Barreno, B., Loópez, D., Melero, J. A., and Del, V. M. (2012) Exogenous, TAP-independent lysosomal presentation of a respiratory syncytial virus CTL epitope. *Immunol. Cell Biol.* **90,** 978–982
28. Trombetta, E. S., and Mellman, I. (2005) Cell biology of antigen processing *in vitro* and *in vivo. Annu. Rev. Immunol.* **23,** 975–1028
29. Barik, S. (1992) Transcription of human respiratory syncytial virus genome RNA in vitro:Requirement of cellular factor(s). *J. Virol.* **66,** 6813–6818
30. Lamb, R. A. (2013) Mononegavirales. In *Fields Virology*, Knipe, D. M., and Howley, P. M., eds. Lippincott Williams & Wilkins, Philadelphia, PA.,
31. Wu, W., Tran, K. C., Teng, M. N., Heesom, K. J., Matthews, D. A., Barr, J. N., and Hiscox, J. A. (2012) The interactome of the human respiratory syncytial virus NS1 protein highlights multiple effects on host cell biology. *J. Virol.* **86,** 7777–7789
32. Tripp, R. A., Hou, S., Etchart, N., Prinz, A., Moore, D., Winter, J., and Anderson, L. J. (2001) CD4(+) T cell frequencies and Th1/Th2 cytokine patterns expressed in the acute and memory response to respiratory syncytial virus I-E(d)-restricted peptides. *Cell Immunol.* **207,** 59–71
33. Eisenlohr, L. C. (2013) Alternative generation of MHC class II-restricted epitopes: Not so exceptional? *Mol. Immunol.* **55,** 169–171
34. Homann, H. E., Hofschneider, P. H., and Neubert, W. J. (1990) Sendai virus gene expression in lytically and persistently infected cells. *Virology* **177,** 131–140
35. Tokusumi, T., Iida, A., Hirata, T., Kato, A., Nagai, Y., and Hasegawa, M. (2002) Recombinant Sendai viruses expressing different levels of a foreign reporter gene. *Virus Res.* **86,** 33–38